

**Photoluminescent diamond nanoparticles for cell labeling:
study of the uptake mechanism in mammalian cells**

Journal:	ACS Nano
Manuscript ID:	nn-2009-01014j.R1
Manuscript Type:	Article
Date Submitted by the Author:	
Complete List of Authors:	<p>Faklaris, Orestis; Ecole Normale Supérieure de Cachan, Laboratoire de Photonique Quantique et Moléculaire JOSHI, Vandana; Université Evry-Val-d'Essonne, INSERM U829 Eirinopoulou, Theano; Institut du Fer à Moulin, Université Pierre et Marie Curie, INSERM UMR-S 839 Tauc, Patrick; Ecole Normale Supérieure de Cachan, Laboratoire de Biologie et de Pharmacologie Appliquée Sennour, Mohamed; Ecole des Mines de Paris, Centre des Matériaux Pierre-Marie Fourt Girard, Hugues; CEA, LIST, Diamond Sensor Laboratory Gesset, Céline; CEA, LIST, Diamond Sensor Laboratory ARNAULT, Jean-Charles; CEA, LIST, Diamond Sensor Laboratory Thorel, Alain; Ecole des Mines de Paris, Centre des Matériaux Pierre-Marie Fourt Boudou, Jean-Paul; Université Evry-Val-d'Essonne, INSERM U829 Curmi, Patrick; Université d'Evry-Val d'Essonne, INSERM U829 Treussart, Francois; Ecole Normale Supérieure de Cachan, Laboratoire de Photonique Quantique et Moléculaire</p>



1
2
3
4
5
6
7
8
9
10
11
12
13
14
15
16
17
18
19
20
21
22
23
24
25
26
27
28
29
30
31
32
33
34
35
36
37
38
39
40
41
42
43
44
45
46
47
48
49
50
51
52

Photoluminescent diamond nanoparticles for cell labeling: study of the uptake mechanism in mammalian cells

Orestis Faklaris,[†] Vandana Joshi,[‡] Theano Irinopoulou,[¶] Patrick Tauc,[§]
Mohamed Sennour,^{||} Hugues Girard,[⊥] Céline Gesset,[⊥] Jean-Charles Arnault,[⊥]
Alain Thorel,^{||} Jean-Paul Boudou,[‡] Patrick A. Curmi,^{*,‡} and François Treussart^{*,†}

Laboratoire de Photonique Quantique et Moléculaire, Ecole Normale Supérieure de Cachan and CNRS UMR 8537, Cachan, France, Laboratoire Structure et Activité des Biomolécules Normales et Pathologiques, Université d'Evry-Val-d'Essonne and INSERM U829, Evry, France, Institut du Fer à Moulin, Université Pierre et Marie Curie and INSERM, UMR-S 839, Paris, France, Laboratoire de Biologie et de Pharmacologie Appliquée, Ecole Normale Supérieure de Cachan and CNRS UMR 8113, Cachan, France, Laboratoire Pierre-Marie Fourt, Centre des Matériaux de l'Ecole des Mines de Paris and CNRS UMR 7633, Evry, France, and Diamond Sensor Laboratory, CEA-LIST, Gif-sur-Yvette, France

[†]CNRS UMR 8537

[‡]INSERM U829

[¶]INSERM UMR-S 839

[§]CNRS UMR 8113

^{||}CNRS UMR 7633

[⊥]CEA-LIST

Abstract

Diamond nanoparticles (nanodiamonds) have been recently proposed as new labels for cellular imaging. For small nanodiamonds (size < 40 nm) resonant laser scattering and Raman scattering cross-sections are too small to allow single nanoparticle observation. Nanodiamonds can however be rendered photoluminescent with a perfect photostability at room temperature. Such a remarkable property allows easier single-particle tracking over long time-scales. In this work we use photoluminescent nanodiamonds of size < 50 nm for intracellular labeling and investigate the mechanism of their uptake by living cells. By blocking selectively different uptake processes we show that nanodiamonds enter cells mainly by endocytosis and converging data indicate that it is clathrin mediated. We also examine nanodiamonds intracellular localization in endocytic vesicles using immunofluorescence and transmission electron microscopy. We find a high degree of colocalization between vesicles and the biggest nanoparticles or aggregates, while the smallest particles appear free in the cytosol. Our results pave the way for the use of photoluminescent nanodiamonds in targeted intracellular labeling or biomolecule delivery.

Key words: diamond, nanoparticles, photoluminescence, biolabel, endocytosis

Introduction

Solid-state nanoparticles hold great promises for biomedical applications, notably thanks to the possibility to combine biological and inorganic materials with the prospect to develop innovative diagnostic and therapeutic tools. Among them, nanoparticles like quantum dots,^{1,2} gold nanobeads³ or silicon beads⁴ are used to label biomolecule with high specificity, to track their fate in cultured cells and in organisms or even to deliver bioactive molecules or drugs. Organic dyes and fluorophores are nowadays the most widely used fluorescent labels of biomolecules. However they photobleach rapidly under continuous illumination,⁵ which makes difficult their quantification and long term follow-up. Interestingly, semiconductor nanocrystals, or quantum dots (QDs),

1
2
3
4 have a better stability and a lower photobleaching yield than organic dyes. They also offer the pos-
5
6 sibility of multicolor staining by size tuning.² On the other hand, such nanoparticles present major
7
8 drawbacks, such as a potential cytotoxicity on long-term scale due to the chemical composition of
9
10 their core⁶ or the intermittency of their photoluminescence (photoblinking) which makes difficult
11
12 an efficient tracking of individual nanoparticles.⁷

13
14 Compared to these nanoparticles, photoluminescent nanodiamonds (PNDs) appear as promis-
15
16 ing alternative biomarkers. Their photoluminescence, with emission in the red and near infrared
17
18 spectral region (575-750 nm) results from nitrogen-vacancy (NV) color centers embedded in the
19
20 diamond matrix.⁸ These emitters present a perfect photostability with no photobleaching nor pho-
21
22 toblinking, and a photoluminescence intensity at saturation which is only three times smaller than
23
24 that of a single commercial QD, a situation which can be reversed in favor of NDs by the use of par-
25
26 ticles containing a large number of color centers.⁹ Such remarkable photoluminescent properties
27
28 have made possible long-term single particle tracking in living cells.⁹⁻¹¹

29
30 Moreover, thanks to a large specific surface area, the nanodiamond can be used as a plat-
31
32 form to graft a large variety of bioactive moieties¹²⁻¹⁵ with the perspective to use these particles
33
34 for instance as intracellular compartment labels¹⁶ or as long term traceable delivery vehicles for
35
36 biomolecule translocation in cell.^{14,15,17,18} Considering the recent demonstrations of PNDs mass
37
38 production,^{11,19} and the numerous experiments showing their low cytotoxicity,^{17,20-22} one can en-
39
40 vision large scale applications of these biolabels. However, such outstanding prospects require a
41
42 better understanding of the mechanism underlying their cellular uptake.

43
44 To that end, we study in the present work the cellular fate of photoluminescent nanodiamonds
45
46 of size <50 nm. We first show that for such a small size nanodiamond, excitation-laser scattering
47
48 yields no signal and that only photoluminescence allows their detection with a sufficiently high
49
50 signal-to-background ratio. We then carry out a systematic investigation of the cellular uptake and
51
52 pathway of PNDs in human cancer cells (HeLa cells) and observe that the internalization of PNDs
53
54 stems mainly from endocytosis. The localization of PNDs in cells is studied using simultaneous
55
56 detection of PNDs and immunofluorescence methods to label the endosomes and the lysosomes.
57
58
59
60

Results and discussion

Nanodiamond observation at the single particle level in cells

In the present work, we use nanodiamonds produced by milling of 150-200 μm diamond microcrystals after the activation of their photoluminescence by the creation of NV color centers in the diamond matrix (see Materials and Methods). We then selected by differential centrifugations of an aqueous suspension of the milled product, a subset of nanodiamonds having a mean hydrodynamic diameter centered on 46 nm. Since diamond refractive index value of 2.4 is about twice larger than that of the cellular medium, diamond can yield a higher back-scattered intensity of the excitation laser light than the cell compartments. Such a scattering signal can then be used to image nanodiamonds in cell with a good contrast.^{10,23} However, the scattering intensity decreases rapidly with the particle size, due to its sixth order dependence on the particle diameter (Rayleigh scattering). It was shown that the smallest nanodiamonds detectable by this technique have sizes of 37 nm.²⁴

Accordingly, we observe that NDs size is too small to image the particles in cell by back-scattered light with a reasonably high signal-to-background ratio which can compete with that of the photoluminescence signal. Figure 1 shows a HeLa cell imaged with a standard confocal microscope (Leica TCS SP2) in three different contrast modes: (a) backscattering (sometimes referred as the “reflection” mode) of the incident laser operating in cw regime at an excitation wavelength of 488 nm, (b) photoluminescence excited by the same laser and detected in the NV color center spectral region and (d) DIC (Differential Interference Contrast) obtained in transmission under white light illumination of the sample. Two PNDs are detected by the different contrast modes and probably correspond to particles bigger than 50 nm (orange arrows pointing to the right on Figure 1c). On the contrary, a few PNDs are only detected in the fluorescence mode (three of them are marked with yellow arrows pointing to the left on Figure 1c). Complementary observations done with a home-made confocal microscope having single color-center sensitivity (Figure S1 of the Supporting Information) confirm this result (Figure S2). These experiments indicate that fluo-

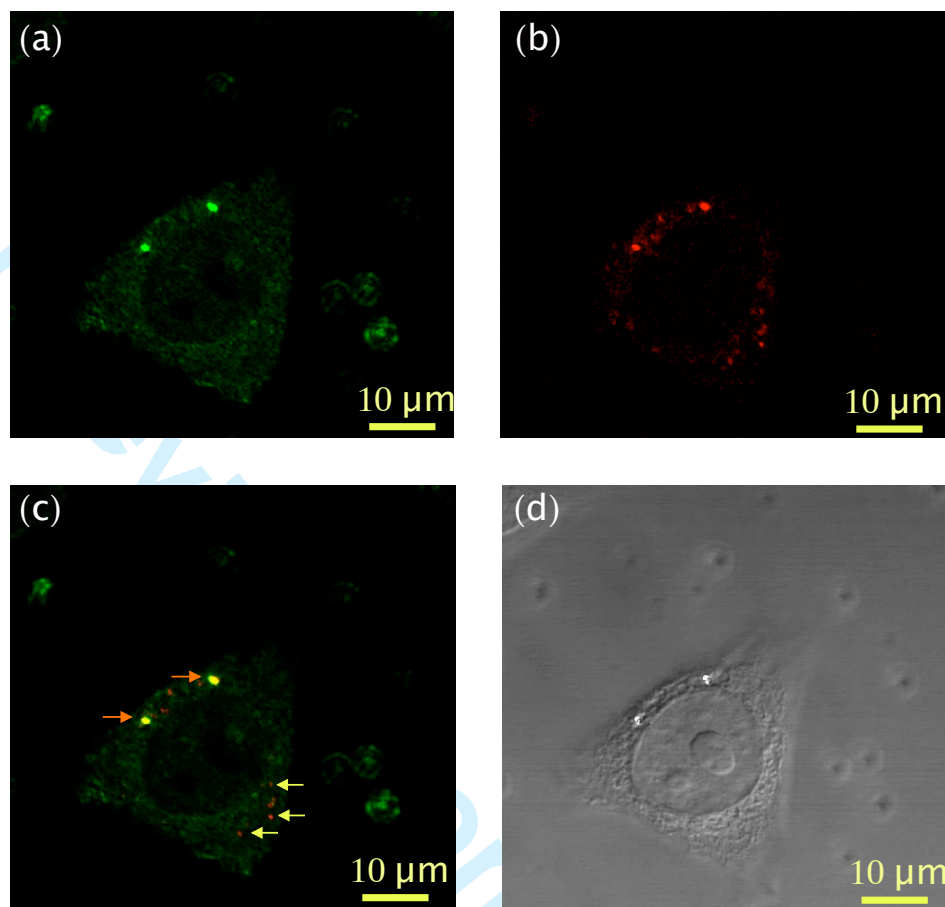


Figure 1: Imaging of photoluminescent nanodiamonds internalized in HeLa cells in three different contrast modes of a Leica TCS SP2 microscope: (a) raster-scan of back-scattered excitation laser light (wavelength 488 nm). (b) photoluminescence confocal raster-scan in the NV color center emission spectrum region (*red channel*, refer to Materials and Methods). (c) overlay of (a) and (b): orange arrows, pointing to the right, exhibit nanoparticles that are observed in both backscattered and fluorescence modes, while the yellow arrows pointing to the left show some nanodiamonds that are detected only in the photoluminescence mode; (d) DIC image obtained in transmission with white light illumination. The confocal section (b) was acquired with laser focusing into the plane located $2.5 \mu\text{m}$ above the coverglass surface on which the cell was grown (image #5 of the cross-section series of Figure S4b).

rescence microscopy is the most appropriate method to detect the smallest PNDs internalized by cells. Moreover, a higher PNDs photoluminescence intensity can be achieved by increasing the number of color centers created per particle. A recent report on PNDs produced a technique similar to the one used here shows that, by optimizing the NV color center creation, one can reach a concentration up to 12 NV centers in nanodiamonds of size around 10 nm.¹⁹ Such a result is very

1
2
3
4 promising for the tracking of very small PNDs in cell.
5
6

7 **Mechanism of PNDs uptake by cells**

8

9
10 It is well established that NDs can spontaneously enter cultured cells, as demonstrated by confocal
11 microscopy^{14,20,21} (Figure S4). In this work we further investigated the internalization mechanism
12 of PNDs in HeLa cells.
13
14

15 We quantified the dynamics of the PNDs uptake by cells by monitoring the overall cell flu-
16 orescence intensity (refer to Materials and methods) and we found that the uptake follows an
17 exponential behavior with time, with a characteristic uptake half-life of 2.6 h (Figure S3). This
18 measurement is compatible with the 3 h uptake half-life observed for 70 nm PNDs²⁵ and the 1.9 h
19 reported for 50 nm gold nanoparticles.²⁶
20
21

22 Endocytosis is considered as the dominant uptake mechanism of extracellular materials of size
23 up to about 150 nm.^{27,28} We therefore evaluated the contribution of endocytosis to NDs internaliza-
24 tion by HeLa cells. For this purpose, the cells were incubated with PNDs (concentration 20 $\mu\text{g/ml}$)
25 under different conditions: (i) at 37°C (control), (ii) at 4°C and (iii) after pretreatment with NaN_3 .
26 The latter treatment disturbs the production of ATP and blocks the endocytosis²⁹ which is an
27 energy-dependant process. Incubation of the cells at 4°C is also known to block endocytosis.
28
29

30 For the analysis of NDs uptake under different cellular treatments, we used the Leica TCS SP2
31 confocal microscope. Figure 2 shows that when endocytosis is hindered by low temperature or
32 NaN_3 , the photoluminescence signal from PNDs strongly decreases (Figure 2b,c) compared to the
33 control (Figure 2a). Similar results were obtained using the home-built confocal microscope which
34 is able to detect all PNDs, including those containing only a single color center, presumably the
35 smallest nanoparticles (Figure S5). These observations, together with the fact that the majority
36 of the NDs from the sample exhibit some photoluminescence (Figure 5, Materials and methods),
37 strongly suggest that very few NDs are internalized when endocytosis is blocked.
38
39

40 To further document the endocytosis mechanisms involved in the cellular uptake of nanodi-
41 amonds, we investigated the receptor-mediated endocytosis (RME) pathway. In RME a ligand
42
43
44
45
46
47
48
49
50
51
52
53
54
55
56
57
58
59
60

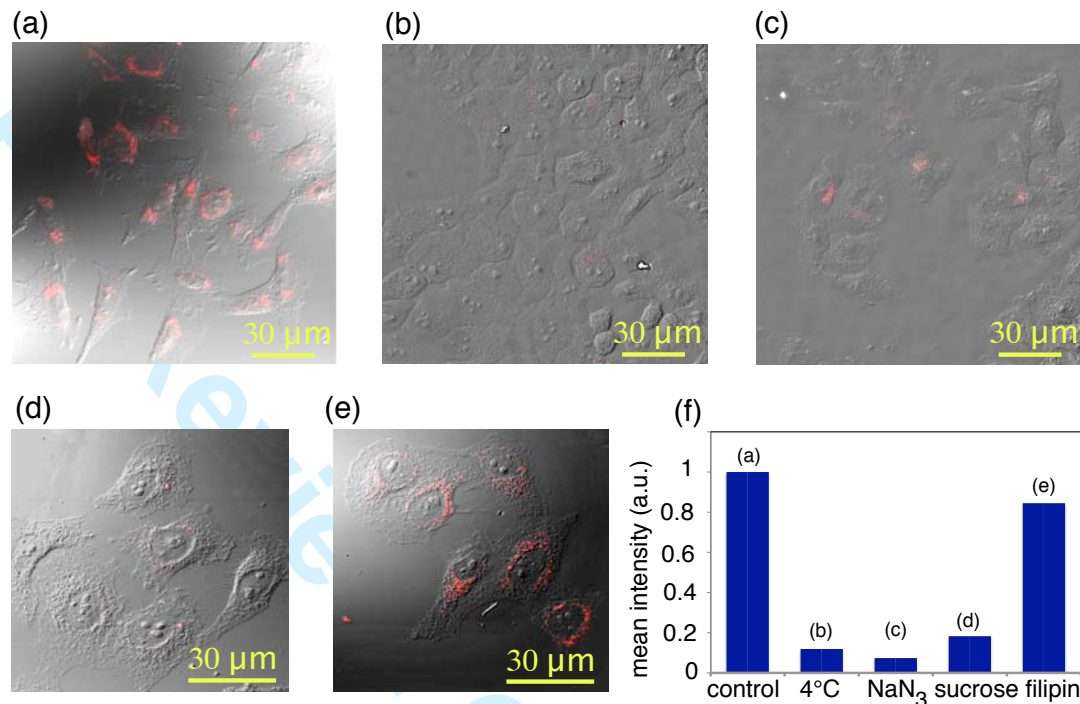


Figure 2: Nanodiamonds are uptaken by HeLa cells through endocytosis. Merged photoluminescence confocal raster scans (*red channel*) and DIC images of PNDs (concentration 20 μg/ml) incubated for 2 hours with cells (a) at 37°C (control) and (b) at 4°C, or at 37°C but after pretreatment with either (c) NaN₃ (10 mM), or (d) sucrose (0.45 M), or (e) filipin (5 μg/ml). Confocal scans are acquired at $z = 1.5 \mu\text{m}$ above the coverglass surface, laser excitation power: 0.5 mW. (f) Mean photoluminescence intensity per cell (in the *red channel*) for the different cell treatments, normalized to the one of control cells and evaluated as described in Materials and Methods.

first binds to a cell surface receptor and is then internalized through an invagination of the plasma membrane. Among the different RME processes, the clathrin mediated pathway is the most frequent one. Clathrin is a protein which coats cell membrane invaginations leading to the budding of clathrin-coated vesicles.^{30,31} Other main RME processes, which are clathrin-independent, occur through the caveolae pathway. Caveolae are invaginations rich in cholesterol.³² In our experiments, cells were incubated with PNDs under conditions that inhibit either the clathrin or the caveolae pathways. Interestingly, we observe that pretreatment of cells with sucrose, a hypertonic treatment known to disrupt the formation of clathrin-coated vesicles,^{33,34} reduces to a high degree the PNDs uptake (Figure 2d). To block the caveolae pathway, cells were pretreated with filipin which disrupts the formation of the cholesterol domains.^{34,35} In contrast to the clathrin-pathway

1
2
3
4 blocking experiment, we observe that pretreatment with filipin does not hinder the internalization
5 of PNDs (Figure 2e). These results indicate that PNDs are mainly internalized by cells by the
6 clathrin-mediated pathway.
7
8

9
10 For a more quantitative analysis, we evaluated the mean photoluminescence intensity per cell
11 (in the *red channel*, corresponding to NV color center emission), in a way similar to the one used
12 for the dynamic measurement of PNDs cellular internalization. Figure 2f shows the change of
13 the mean photoluminescence intensity per cell, normalized to that of control cells. This graph
14 summarizes quantitatively the effects of the different cell treatments, and supports the conclusion
15 that the uptake mechanism of PNDs is endocytosis, with strong indications that it is clathrin medi-
16 ated. The latter statement is reinforced by a complementary analysis done on nanodiamond surface
17 functions. We studied by FTIR spectroscopy the modifications of ND surface functions signatures
18 before and after their mixture with serum supplemented culture medium (refer to Supporting In-
19 formation, Figure S9). We observed that proteins of the serum are adsorbed onto the nanodiamond
20 surface, which may facilitate a receptor-mediated endocytosis. Concomitantly, we noticed that
21 the addition of serum greatly improves the stability of the nanodiamond suspension in the culture
22 medium, which is also related to surface modifications impacting its electric charge.
23
24
25
26
27
28
29
30
31
32
33
34
35

36 The present results on nanodiamond internalization pathway are close to those obtained on the
37 same HeLa cell line for other types of nanoparticles with similar sizes, like gold nanoparticles²⁶
38 or single-walled carbon nanotubes noncovalently conjugated with DNA molecules or proteins.³⁶
39
40
41
42
43

44 **Intracellular localization of PNDs**

45
46 After an endocytic uptake, the internalized compound is expected to be found in intracellular en-
47 dosomal and lysosomal vesicles, before eventually being released in the cytosol or expelled from
48 the cell. Endosomes are vesicles involved in the transport of extracellular materials in the cell
49 cytoplasm. After internalization, endosomes are either recycled to the plasma membrane and the
50 receptors can be used for a novel cycle or they are fused with lysosomes.³⁰
51
52
53
54
55
56

57 In a previous study we concluded from immunofluorescence analyses that 25 nm PNDs are
58
59
60

partially colocalized with early endosomes.²¹ Here we provide similar but more complete results obtained with PNDs differently produced. Apart from a difference in the mean size between the two kinds of PNDs, the nanoparticles have not the same morphologies as it can be seen on TEM images (Figure 5c and also Ref.¹⁹): the shape of the 46 nm nanoparticles produced by milling is more spherical, while the 25 nm commercial NDs present sharper edges.³⁷ These differences may impact the uptake efficiency and justify a new localization study.

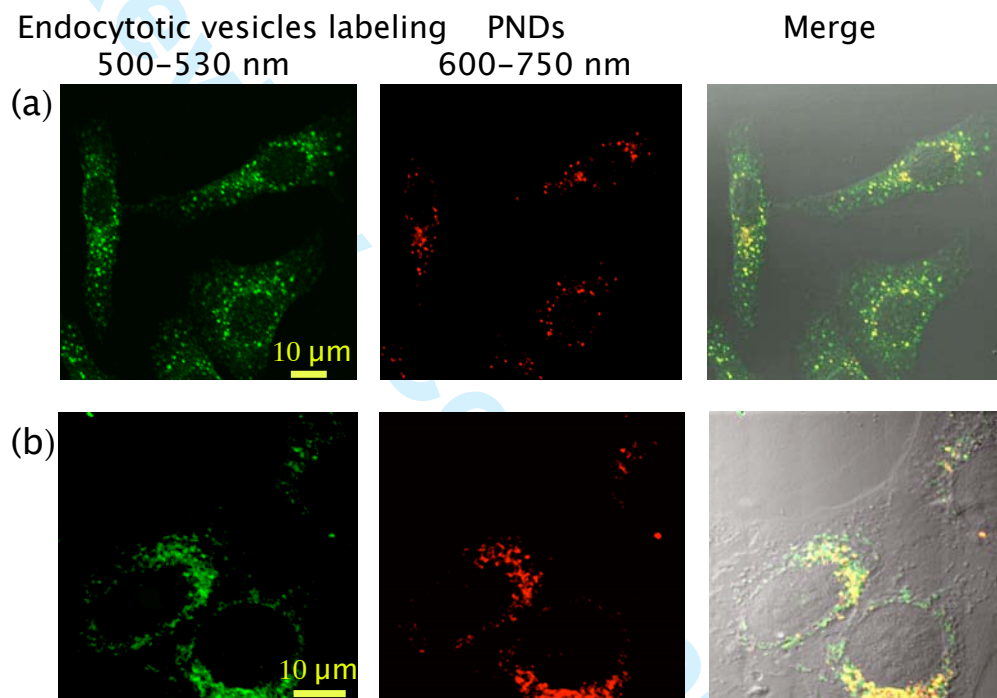


Figure 3: Localization of 46 nm photoluminescent nanodiamonds in HeLa cells. Confocal fluorescence raster-scan (Leica TCS SP2 microscope) of HeLa cell incubated with PNDs ($10 \mu\text{g/ml}$) in normal (control) conditions, then fixed and labeled with endosomes or lysosomes dyes. From left to right: raster-scan in the *green channel* (500-530 nm) showing the endocytic compartments; in the *red channel* (600-750 nm) showing the PNDs. Images on the right represent the merged the green and red scans. (a) Colocalization study of PNDs with early endosomes labeled with EEA1-FITC fluorescent conjugate. (b) Colocalization of PNDs with lysosomes labeled with LysoTracker Green dye. PNDs colocalized with endosomes or lysosomes appear in yellow in the merged fluorescence scans.

Early endosomes and lysosomes were marked with fluorescent labels emitting in the green spectral region (500-550 nm), with no overlap with the red and near infrared emission of NV color centers (Figure 5d). Scanning confocal imaging was carried out with the Leica TCS SP2

1
2
3
4
5
6
7
8
9
10
11
12
13
14
15
16
17
18
19
20
21
22
23
24
25
26
27
28
29
30
31
32
33
34
35
36
37
38
39
40
41
42
43
44
45
46
47
48
49
50
51
52
53
54
55
56
57
58
59
60

microscope. The *red channel* detection spectral range selected for PNDs imaging is 600-750 nm to avoid again any overlap with the emission of the cellular components labels (see Figure S6 for a control experiment). Figure 3 shows a high degree of colocalization of PNDs with both early endosomes and lysosomes, which supports the fact that NDs follow the course of the endocytic cycle. This endosomal localization of PNDs again agrees with reports on other kind of similar size nanoparticles, like QDs³⁸ or gold nanobeads.^{26,39}

To further elucidate the fate of the smallest and less bright PNDs that cannot be detected with the Leica TCS SP2 microscope, we examined the same samples with two complementary techniques: with the home-built confocal setup (Figure S1) detecting the smallest photoluminescent PNDs and with electron microscopy. Observations with the home-built confocal microscope show a partial colocalization (Figure S7), which is also confirmed by Transmission Electron Microscopy (TEM) imaging. In the latter technique, NDs particles appear as dark spots on the grey cytoplasmic background⁴⁰.

In the large scale TEM image (Figure 4a) of a part of a HeLa cell incubated with PNDs, one can observe the nanoparticles in the cytoplasm. They are either trapped in vesicles (Figure 4b,f), or free in the cytosol (Figure 4d and Figure S8b). NDs trapped in vesicles form aggregates (Figure 4b and Figure S9a), and represent the majority of the nanodiamonds observed by TEM inside the cell cytoplasm. This is in agreement with our colocalization studies and with the confined motion of PNDs observed with wide-field microscopy.^{11,21} Nanodiamonds which are free in the cytosol correspond to the smallest particles that can be observed at their primary size (<5-10 nm) or as small aggregates of a few particles. These free nanoparticles have either been released from the endosomes or may have been directly internalized *via* passive transport (like facilitated diffusion) through the cell membrane. Interestingly, all internalized nanodiamonds, even of the smallest size (<5 nm) are observed in perinuclear regions and none of them seems to be present inside the nucleus.

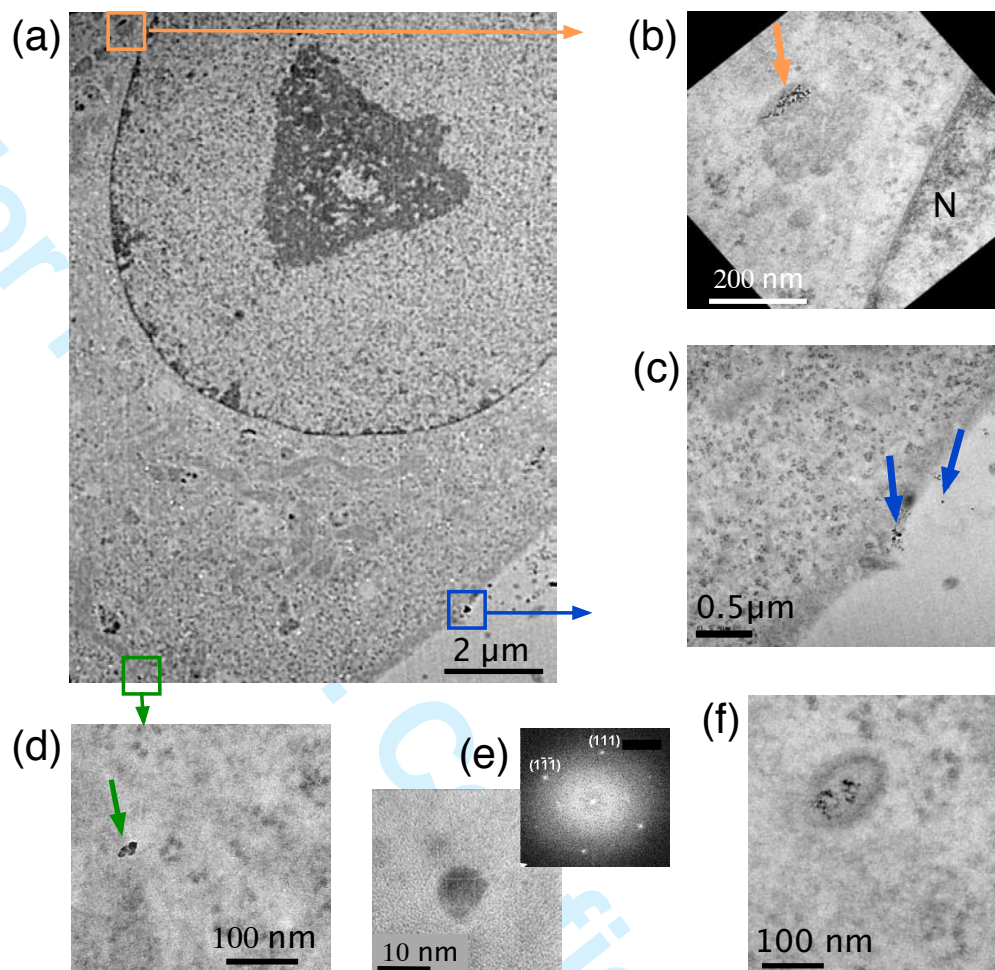


Figure 4: Transmission Electron Microscopy images of a HeLa cell incubated with PNDs for 2 hours. (a) Large scale image. (b) NDs trapped in intracellular vesicles, N indicates the position of cell nucleus. (c) NDs outside the cell and on the cell membrane (blue arrows), probably during the early stage of the internalization process, since the half-life uptake (2.6 hours) is longer than the incubation time. (d) free NDs in the cytoplasm. (e) zoom on one 10 nm ND, inset : local area Fourier transform diffractogram of this ND. (f) PNDs trapped in an intracellular vesicle of another cell from the same sample.

Conclusion

In this work we used 46 nm mean size photoluminescent diamond nanoparticles produced by micron-size diamond milling as cell labels. We showed that photoluminescence detection allows imaging the smallest nanodiamonds that cannot be observed by the backscattered light of the excitation laser. This result underlines the superiority of photoluminescence for tiny nanodiamonds

1
2
3
4
5
6
7
8
9
10
11
12
13
14
15
16
17
18
19
20
21
22
23
24
25
26
27
28
29
30
31
32
33
34
35
36
37
38
39
40
41
42
43
44
45
46
47
48
49
50
51
52
53
54
55
56
57
58
59
60

imaging in complex environments such as the intracellular medium. With the use of a commercial laser scanning confocal microscope, we showed that the internalization of PNDs in HeLa cells occurs through endocytosis and we have strong indications that it is receptor-mediated *via* the clathrin pathway.

We observed that most of the nanodiamonds are localized in intracellular endocytic vesicles in the perinuclear region, except for a small portion, in particular the smallest particles, that appear to be free in the cytoplasm. The later maybe of interest for biomolecule delivery applications, owing to its high diffusion coefficient in the cytosol. However, as cell represents an inhomogeneous medium, a more detailed understanding of the distribution of nanoparticles in the cytoplasm is only the first step towards the utilization of diamond nanoparticles for biological applications (translocation and tracking of biomolecules in cell, labeling of specific compartments or tumorous cells, etc...). The observations reported in this article deserve to be complemented with correlations between intracellular localization and size, shape, surface chemistry and incubation time of nanodiamonds with cells.

Finally, while small PNDs, free in the cytosol are ideal candidates for biomolecules transport and/or specific labeling of cellular compartments, big nanoparticles could serve as whole cell labels, due to their high uptake efficiency²⁶ and their strong photoluminescence or back-scattering light signal. Following this strategy, 100 nm in size nanodiamonds were very recently used for labeling and tracking of cell division and differentiation in cancer and stem cells.⁴¹

Materials and Methods

Production and characterization of Photoluminescent NanoDiamonds (PNDs)

The PNDs production is described in details in Ref.¹⁹. Briefly, the starting material was type Ib diamond synthetic micron size powder (Element Six, The Netherlands) with a specified size of 150-200 μm . NV centers were created by electron irradiation (irradiation dose $2 \times 10^{18} \text{ e}^-/\text{cm}^2$, beam energy 8 MeV) and subsequent annealing (800°C, 2 h) in vacuum (pressure $\simeq 10^{-8}$ mbar).

1
2
3
4 Diamond microcrystals were then reduced in size by nitrogen jet milling to obtain submicron size
5 crystals (Hosokawa-Alpine, Germany). Further size reduction to nanoparticles was achieved by
6 ball milling under argon (Fritsch, Germany). The milled powder was then sieved and treated by
7 strong sonication (60 min at 50°C), followed by acid treatment. After rinsing with pure water,
8 filtration and centrifugation, we obtained PNDs with an average hydrodynamic diameter of 46 nm
9 in a stable water suspension. The size measurement was done by dynamic light Scattering (DLS)
10 corrected from Mie scattering, using the DL135 particle size analyzer (Cordouan Technologies,
11 France). The associated zeta potential of this solution was -43 mV (Zetasizer Nano ZS from
12 Malvern, UK).
13
14
15
16
17
18
19
20
21

22 To simultaneously characterize the PNDs in size and photoluminescence intensity, we used
23 an Atomic Force Microscope (AFM, MFP-3D Asylum Research, USA) coupled to a home-built
24 confocal microscope setup similar to the one depicted on Figure S1 (Supporting Information).
25 For such a study, a droplet of the PND aqueous suspension was deposited by spin-coating on a
26 glass coverslip which was then simultaneously imaged in AFM (Figure 5a) and photolumines-
27 cence (Figure 5b) modes. Among 200 nanodiamonds identified on the AFM scan, 115 display a
28 photoluminescence signal, i.e. about 58% of the NDs are photoluminescent. Among the photolu-
29 minescent nanoparticles a small fraction consists of 10-15 nm diameter PNDs, but the majority of
30 the PNDs appears as nano-objects of size 40-50 nm. Some of them form aggregates of 2-3 smaller
31 particles, as can be inferred from TEM imaging (Figure 5c).
32
33
34
35
36
37
38
39
40
41
42
43

44 **Photoluminescence and backscattered light imaging of nanodiamonds**

45
46
47 The large scale photoluminescence observations of PNDs in the cells which are presented in the
48 main text are done with a commercial Leica TCS SP2 (Manheim, Germany) laser scanning con-
49 focal microscope, with a $\times 63$, 1.4 numerical aperture (NA) oil-immersion objective. Excitation
50 comes from the cw argon ion laser line at 488 nm wavelength. We use one Airy Unit as the pinhole
51 diameter, for all the acquisitions. The detection was done in two non-overlapping spectral chan-
52 nels: *green channel* (500-530 nm) collecting the fluorescence from FITC and LysoTracker-green
53
54
55
56
57
58
59
60

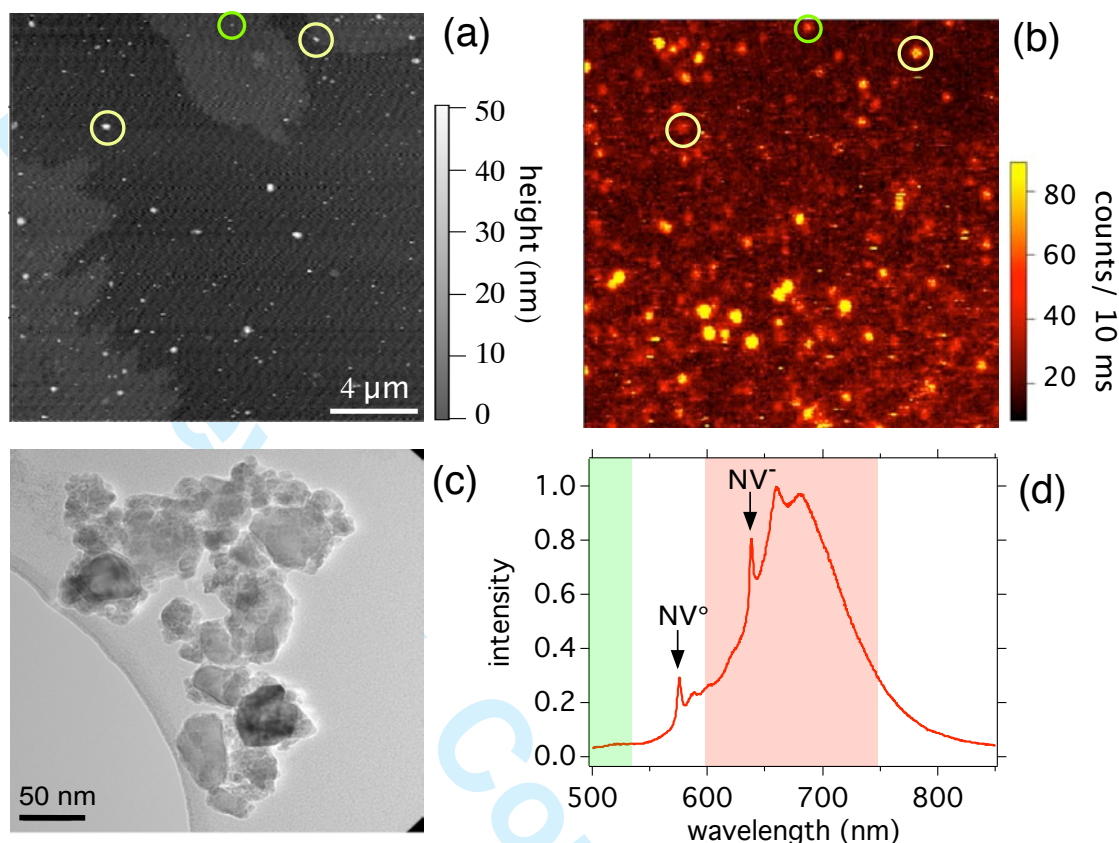


Figure 5: Simultaneous size and photoluminescence characterization of the PNDs used in this work. Sample is a coverglass on which an aqueous suspension of PNDs is deposited by spin-coating. (a) and (b): raster scans ($18 \times 18 \mu\text{m}$) of the same region of the sample in the two modes (a) AFM and (b) confocal microscopy. For confocal imaging, the excitation laser wavelength is 532 nm, at an excitation power of $200 \mu\text{W}$, and the photoluminescence intensity scale bar maximum of graph (b) was set to 90 counts/10 ms in order to be able to observe the less intense PNDs (the brightest spot yields 367 counts/10 ms). Two nanodiamonds of height ~ 40 nm are circled in yellow, while a 12 nm height nanodiamond is inside the green circle, still displaying a strong photoluminescence signal. (c) High-Resolution TEM image of the same type of PNDs. A droplet of the aqueous suspension was initially dried on the carbon grid. (d) Photoluminescence spectrum of NV color centers embedded in the starting micron-size diamond crystal (after irradiation and before milling). The narrow lines pointed out by arrows at 575 nm and 637 nm indicate respectively the zero-phonon lines of the neutral NV° and negatively charged NV^- color centers, present in this sample. The light red/green rectangles behind NV spectra indicates the spectral range selected by the *red/green channels* filters respectively on the Leica TCS SP2 microscope for PNDs.

dye conjugates, and the red channel (600-750 nm) collecting mainly NV^- photoluminescence (see Figure 5d).

For the single particle analysis presented in the Supporting Information, the photoluminescence

1
2
3 was probed using a home-built scanning-stage confocal microscope. It relies on a Nikon TE300
4 microscope, converted to a confocal setup with the appropriate modifications (refer to Figure S1 of
5 Supporting Information for more details). The microscope objective used is a $\times 60$, 1.4 numerical
6 aperture (NA) apochromatic oil immersion objective. The excitation is a cw laser emitting at the
7 wavelength of 488 nm. The photoluminescence signal was acquired by an avalanche photodiode
8 in the single-photon counting mode. This home-built confocal setup is sensitive to the photolu-
9 minescence of a single NV color center in a PND, in a cultured cell environment.²¹ To record
10 the backscattered excitation laser light, we used a properly oriented quarter-wave plate and po-
11 larizing beam-splitter cube assembly to redirect all the reflected light towards an other avalanche
12 photodiode in the single-photon counting mode.
13
14
15
16
17
18
19
20
21
22
23

24 For the PNDs uptake kinetics study, we estimated from the confocal raster scans the mean
25 fluorescence intensity per cell in the red channel. For this purpose we used the *mean intensity*
26 analysis/measure tool of *ImageJ* software (NIH, USA). About 40 cells were analyzed for each
27 different incubation time.
28
29
30
31
32
33

34 **Cell culture conditions and test of nanodiamond cytotoxicity**

35
36 HeLa cells were grown in standard conditions on glass coverslips in Dulbecco modified Eagle
37 medium (DMEM) supplemented with 10% fetal calf serum (FCS) and 1% penicillin/streptomycin.
38 To study the cellular uptake of PNDs, cells were seeded at a density of 2×10^5 cells/ 1.3 cm^2 and
39 grown at 37°C in a humidified incubator under 5% CO_2 atmosphere. 24 h after seeding, the PNDs
40 aqueous suspension was added to the cell culture medium. The cells were grown under similar
41 conditions for an additional period of time (from 2 h for fluorescence examination, up to 24 h for
42 the cytotoxicity tests). After incubation, the excess of PNDs was removed by washing the cells with
43 phosphate buffer saline (PBS). The cells were then fixed with 4% paraformaldehyde in PBS and
44 mounted on microscope slides for phase contrast and confocal microscopy studies. A necessary
45 requirement to use PNDs as biomolecule markers is their low cytotoxicity. As cytotoxicity depends
46 on the cellular type used and the size, shape and charge of the nanoparticles,⁴² we performed
47
48
49
50
51
52
53
54
55
56
57
58
59
60

1
2
3
4
5
6
7
8
9
10
11
12
13
14
15
16
17
18
19
20
21
22
23
24
25
26
27
28
29
30
31
32
33
34
35
36
37
38
39
40
41
42
43
44
45
46
47
48
49
50
51
52
53
54
55
56
57
58
59
60

cytotoxicity tests for the PNDs used here. We show that they are not toxic *in vitro* after 24 h of incubation with cells (Figure S10).

Cellular uptake of nanodiamonds

To investigate the **uptake mechanism of PNDs**, cells were treated as follows:

Experiments blocking the endocytosis (energy dependent process): for low temperature incubation, cells were grown as described above with the cell culture kept at 4°C instead of 37°C. For the incubation with PNDs under ATP depletion, the cells were preincubated in PBS buffer, supplemented with 10 mM NaN₃ during 30 min at 37°C and then PNDs were added.

For the **investigation of the type of receptor-mediated endocytosis mechanism**, cells were treated as follows:

Hypertonic treatment to hinder the clathrin-mediated process: the cells were pre-incubated for 30 min in PBS buffer supplemented with 0.45 M sucrose followed by incubation with PNDs at 37°C.

Filipin treatment blocking caveolae pathway: the cells were pretreated in PBS buffer, supplemented with filipin (5 µg/ml) for 30 min before exposure to PNDs at 37°C.

For **PNDs intracellular localization analyses** by immunofluorescence, the endosomes were labeled with FITC-conjugated Mouse Anti-human Early Endosome Antigen EEA1 (Ref. 612006, BD Transduction Laboratories, USA).²¹ FITC dye has absorption/emission maxima at 490/520 nm respectively. The lysosomes were labeled with LysoTracker Green DND-26 dye (L7526, Invitrogen, USA), with absorption/emission maxima at 504/511 nm respectively. After two hours of incubation of PNDs at 37°C with the cells, the medium was replaced with prewarmed new medium containing the LysoTracker probe (75 nM), for one additional hour of incubation. The medium was then replaced with fresh medium just before cell fixation as described above.

Transmission electron microscopy

The electron microscopy observations were done with a High Resolution Transmission Electron Microscope (HR-TEM, Tecnai F20 operating at 200 keV). Cells were seeded for 24 h in standard conditions (conditions similar to those used for fluorescence experiments). PNDs were added in cell culture medium and incubated for 2 h at 37°C. Cells were then fixed in a solution of paraformaldehyde, glutaraldehyde and phosphate buffer for 45 min at room temperature. After dehydration with a graded series of ethanol, the cells were embedded in EPON resin. Ultrathin sections of the resin block were then cut (100 nm thickness) and stained with 2% uranyl acetate, for a higher contrast imaging under the HR-TEM microscope.

Acknowledgement

We are grateful to Jean-François Roch and Karen Perronet for fruitful discussions. We thank Géraldine Dantelle for the measurements of diamond colloidal suspensions zeta potentials and Anne Tarrade for the preparation of the samples observed with Transmission Electron Microscopy. This work was supported by the European Commission through the project "Nano4Drugs" (contract LSHB-2005-CT-019102), by Agence Nationale de la Recherche through the project "NanoDia" (contract ANR-2007-PNANO-045) and by a "Ile-de-France" Region *C'Nano* grant under the project "Biodiam".

Supporting Information Available

The home built scanning confocal microscopy setup is described in Figure S1. This microscope has a single NV color center sensitivity, allowing the observation of the smallest PNDs. It was used for a more precise comparison of the photoluminescence and the backscattered signal coming from PNDs deposited on a glass-coverslip (Figure S2). It was also used for PNDs observation in cultured cell, in particular to show that even the smallest PNDs are not internalized when they are incubated at 4°C with HeLa cells (Figure S5); and finally to make a high sensitivity colocalization

1
2
3
4 study of PNDs with endosomes (Figure S7).

5
6 Additional observations done with the commercial Leica TCS SP2 microscope are given in
7
8 Figure S3 (graph representing the dynamics of photoluminescent nanodiamonds uptake by HeLa
9
10 cells), and Figure S4 (3D-reconstruction of confocal raster scans showing the localization of PNDs
11
12 in the Figure 1 cell). For the colocalization studies, we checked that there is no crosstalk between
13
14 PNDs and FITC detection channels (Figure S6). We also provide additional High-Resolution TEM
15
16 images of a HeLa cell incubated with PNDs (Figure S8).

17
18 The surface function characterization by Fourier Transform Infra Red (FT-IR) spectroscopy
19
20 of nanodiamonds before and after mixture with the foetal calf serum is explained in details with
21
22 spectra provided in Figure S9.

23
24 The cytotoxicity-test results of PNDs incubated with HeLa cells are presented on Figure S10.

25
26 This material is available for download from <http://pubs.acs.org>
27
28
29

30 31 32 33 34 35 36 37 38 39 40 41 42 43 44 45 46 47 48 49 50 51 52 53 54 55 56 57 58 59 60

References

1. Alivisatos, P. The use of nanocrystals in biological detection. *Nat. Biotechnol.* **2004**, *22*, 47–52.
2. Michalet, X.; Pinaud, F.; Bentolila, L.; Tsay, J.; Doose, S.; Li, J.; Sundaresan, G.; Wu, A.; Gambhir, S.; Weiss, S. Quantum Dots for Live Cells, in Vivo Imaging, and Diagnostics. *Science* **2005**, *307*, 538–544.
3. Lasne, D.; Blab, G.; Berciaud, S.; Heine, M.; Groc, L.; Choquet, D.; Cognet, L.; Lounis, B. Single Nanoparticle Photothermal Tracking (SNaPT) of 5-nm Gold Beads in Live Cells. *Biophys. J.* **2006**, *91*, 4598 – 4604.
4. Warner, J.; Hoshino, A.; Yamamoto, K.; Tilley, R. Water-Soluble Photoluminescent Silicon Quantum Dots. *Angew. Chem. Int. Ed.* **2005**, *44*, 4550 – 4554.
5. Resch-Genger, U.; Grabolle, M.; Cavaliere-Jaricot, S.; Nitschke, R.; Nann, T. Quantum dots versus organic dyes as fluorescent labels. *Nat. Meth.* **2008**, *9*, 763–775.

6. Kirchner, C.; Liedl, T.; Kudera, S.; Pellegrino, T.; Javier, A.; Gaub, H.; Stoelze, S.; Fertig, N.; Parak, W. Cytotoxicity of Colloidal CdSe and CdSe/ZnS Nanoparticles. *Nano Lett.* **2005**, *5*, 331.
7. Nirmal, M.; Dabbousi, B.; Bawendi, M.; Macklin, J.; Trautman, J.; Harris, T.; Brus, L. Fluorescence intermittency in single cadmium selenide nanocrystal. *Nature* **1996**, *383*, 802–804.
8. Gruber, A.; Dräbenstedt, A.; Tietz, C.; Fleury, L.; Wrachtrup, J.; Von Borczyskowsky, C. Scanning Confocal Optical Microscopy and Magnetic Resonance on Single Defect Centers. *Science* **1997**, *276*, 2012.
9. Faklaris, O.; Garrot, D.; Joshi, V.; Boudou, J.-P.; Sauvage, T.; Curmi, P. A.; Treussart, F. Comparison of the photoluminescence properties of semiconductor quantum dots and non-blinking diamond nanoparticles and observation of the diffusion of diamond nanoparticles in living cells. *J. Europ. Opt. Soc. Rap. Public.* **2009**, *4*, 09035.
10. Neugart, F.; Zappe, A.; Jelezko, F.; Tietz, C.; Boudou, J.-P.; Krueger, A.; Wrachtrup, J. Dynamics of Diamond Nanoparticles in Solution and Cells. *Nano Lett.* **2007**, *7*, 3588–3591.
11. Chang, Y.-R.; Lee, H.-Y.; Chen, K.; Chang, C.-C.; Tsai, D.-S.; Fu, C.-C.; Lim, T.-S.; Tzeng, Y.-K.; Fang, C.-Y.; Han, C.-C.; *et al.*, Mass production and dynamic imaging of fluorescent nanodiamonds. *Nat. Nanotechnol.* **2008**, *3*, 284–288.
12. Krüger, A. Diamond nanoparticles for biological applications. *J. Chem. Eur.* **2008**, *14*, 1382.
13. Liang, Y.; Ozawa, M.; Krüger, A. A General Procedure to Functionalize Agglomerating Nanoparticles Demonstrated on Nanodiamond. *ACS Nano* **2009**, DOI: 10.1021/nn900339s.
14. Chao, J.-I.; Perevedentseva, E.; Chung, P.-H.; Liu, K.-K.; Cheng, C.-Y.; Chang, C.-C.; Cheng, C.-L. Nanometer-Sized Diamond Particle as a Probe for Biolabeling. *Biophys. J.* **2007**, *93*, 2199–2208.

- 1
2
3
4
5
6
7
8
9
10
11
12
13
14
15
16
17
18
19
20
21
22
23
24
25
26
27
28
29
30
31
32
33
34
35
36
37
38
39
40
41
42
43
44
45
46
47
48
49
50
51
52
53
54
55
56
57
58
59
60
15. Vial, S.; Mansuy, C.; Sagan, S.; Irinopoulou, T.; Burlina, F.; Boudou, J.-P.; Chassaing, G.; Lavielle, S. Peptide-grafted nanodiamonds: preparation, cytotoxicity and uptake in cells. *ChemBioChem* **2008**, *9*, 2113–2119.
 16. Mkandawire, M.; Pohl, A.; Gubarevich, T.; Lapina, V.; Appelhans, D.; Rödel, G.; Pompe, W.; Schreiber, J.; Opitz, J. Selective targeting of green fluorescent nanodiamond conjugates to mitochondria in HeLa cells. *J. Biophot.* **2009**, DOI: 10.1002/jbio.200910002.
 17. Huang, H.; Pierstorff, E.; Osawa, E.; Ho, D. Active nanodiamond hydrogels for chemotherapeutic delivery. *Nano Lett.* **2007**, *7*, 3305–3314.
 18. Chen, M.; Pierstorff, E.; Lam, R.; Li, S.-Y.; Huang, H.; Osawa, E.; Ho, D. Nanodiamond-Mediated Delivery of Water-Insoluble Therapeutics. *ACS Nano* **2009**, *3*, 2016–2022.
 19. Boudou, J.-P.; Curmi, P. A.; Jelezko, F.; Wrachtrup, J.; Aubert, P.; Sennour, M.; Balasubramanian, G.; Reuter, R.; Thorel, A.; Gaffet, E. High yield fabrication of fluorescent nanodiamonds. *Nanotechnology* **2009**, *20*, 235602.
 20. Fu, C.-C.; Lee, H.-Y.; Chen, K.; Lim, T.-S.; Wu, H.-Y.; Lin, P.-K.; Wei, P.-K.; Tsao, P.-H.; Chang, H.-C.; Fann, W. Characterization and applications of single fluorescent nanodiamonds as cellular biomarkers. *Proc. Nat. Acad. Sc.* **2007**, *104*, 727.
 21. Faklaris, O.; Garrot, D.; Joshi, V.; Druon, F.; Boudou, J.-P.; Sauvage, T.; Georges, P.; Curmi, P. A.; Treussart, F. Detection of single photoluminescent diamond nanoparticles in cells and study of their internalization pathway. *Small* **2008**, *4*, 2236–2239.
 22. Schrand, A. M.; Huang, H.; Carlson, C.; Schlager, J.; Osawa, E.; Hussain, S.; Dai, L. Are diamond nanoparticles cytotoxic? *J. Phys. Chem. B* **2007**, *111*, 2–7.
 23. Smith, B.-R.; Niebert, M.; Plakhotnik, T.; Zvyagin, A.-V. Transfection and imaging of diamond nanocrystals as scattering optical labels. *Journal of Luminescence* **2007**, *127*, 260.

- 1
2
3
4 24. Colpin, Y.; Swan, A.; Zvyagin, A.; Plakhotnik, T. Imaging and sizing of diamond nanoparticles. *Opt. Lett.* **2006**, *31*, 625.
5
6
7
8
9 25. Wee, T.-L.; Mau, Y.-W.; Fang, C.-Y.; Hsu, H.-L.; Han, C.-C.; Chang, H.-C. Preparation and
10 characterization of green fluorescent nanodiamonds for biological applications. *Diam. Rel.*
11 *Mat.* **2009**, *18*, 567–573.
12
13
14
15 26. Chithrani, B.; Ghazani, A.; Chan, W.-C. Determining the Size and Shape Dependence of Gold
16 Nanoparticle Uptake into Mammalian Cells. *Nano Lett.* **2006**, *6*, 662– 668.
17
18
19
20 27. Marsh, M.; McMahon, H. Cell biology - The structural era of endocytosis. *Science* **1999**, *285*,
21 215.
22
23
24
25 28. Murkherjee, S.; Ghosh, R.; Maxfield, F. Endocytosis. *Physiol. Rev.* **1997**, *77*, 759–803.
26
27
28 29. Schmid, S.; Carter, L. ATP is Required for Receptor-mediated Endocytosis in Intact Cells. *J.*
29 *Cell Biol.* **1990**, *111*, 2307–2318.
30
31
32 30. Steinman, R.; Mellman, I.; Muller, W.; Cohn, Z. Endocytosis and the Recycling of Plasma
33 Membrane. *J. Cell Biol.* **1983**, *96*, 1–27.
34
35
36
37 31. Mousavi, S.; Malerod, L.; Berg, T.; Kjekken, R. Clathrin-dependent endocytosis. *Biochem. J*
38 **2004**, *377*, 1–16.
39
40
41
42 32. Pelkmans, L.; Brli, T.; Zerial, M.; Helenius, A. Caveolin-Stabilized Membrane Domains as
43 Multifunctional Transport and Sorting Devices in Endocytic Membrane Traffic. *Cell* **2004**,
44 *118*, 767–780.
45
46
47
48
49 33. Heuser, J.; Anderson, R. Hypertonic media inhibit receptor-mediated endocytosis by blocking
50 clathrin-coated pit formation. *J. Cell Biol.* **1989**, *108*, 389–400.
51
52
53
54 34. Qaddoumi, M.; Gukasyan, H.; Davda, J.; Labhasetwar, V.; Kim, K.; Lee, V. Clathrin and
55 caveolin-1 expression in primary pigmented rabbit conjunctival epithelial cells: Role in PLGA
56 nanoparticle endocytosis. *Molec. Vis.* **2003**, *9*, 559–568.
57
58
59
60

- 1
2
3
4
5
6
7
8
9
10
11
12
13
14
15
16
17
18
19
20
21
22
23
24
25
26
27
28
29
30
31
32
33
34
35
36
37
38
39
40
41
42
43
44
45
46
47
48
49
50
51
52
53
54
55
56
57
58
59
60
35. Kruth, H.; Vaughan, M. Quantification of low density lipoprotein binding and cholesterol accumulation by single human fibroblasts using fluorescence microscopy. *J Lipid Res* **1980**, *21*, 123–130.
36. Kam, N.; Liu, Z.; Dai, H. Carbon Nanotubes as Intracellular Transporters for Proteins and DNA : An Investigation of the Uptake Mechanism and Pathway. *Angew. Chem. Int. Ed.* **2006**, *45*, 577–581.
37. Treussart, F.; Jacques, V.; Wu, E.; Gacoin, T.; Grangier, P.; Roch, J.-F. Photoluminescence of single colour defects in 50 nm diamond nanocrystals. *Physica B* **2006**, *376*, 926–929.
38. Jaiswai, J.-K.; Mattoussi, H.; Mauro, J.; Simon, S.-M. Long-term multiple color imaging of live cells using quantum dot bioconjugates. *Nat. Biotechnol.* **2002**, *21*, 47.
39. Nativo, P.; Prior, I.; Brust, M. Uptake and Intracellular Fate of Surface-Modified Gold Nanoparticles. *ACS Nano* **2008**, *2*, 1639–1644.
40. We checked by carrying out a local area Fourier transform electron diffractogram on one of the TEM dark spots of size $\simeq 10$ nm that it has the signature of diamond material (inset of Figure 4e).
41. K.-K. Liu, C.-L. C., C.-C. Wang; Chao, J.-I. Endocytic carboxylated nanodiamond for the labeling and tracking of cell division and differentiation in cancer and stem cells. *Biomaterials* **2009**, *30*, 4249.
42. Lewinski, N.; Colvin, V.; Drezek, R. Cytotoxicity of Nanoparticles. *Small* **2008**, *4*, 26–49.